Traction System with On-Board Inductive Power Transfer

A. S. Abdel-Khalik[*], *S. Ahmed*[**], *and A. Massoud*[†,*]

* *Alexandria University, Egypt, ayman@spiretronic.com,*
***Texas A&M University at Qatar, Qatar, shehab.ahmed@qatar.tamu.edu*
†*Qatar University, Qatar ahmed.massoud@qu.edu.qa*

Keywords: Linear motor, contactless power transmission, brushless doubly fed machines, mixed pole machines, traction.

Abstract

In traction applications based on long primary and short secondary type, contactless electrical energy transmission can offer distinct advantages over the conventional energy transmission based on catenary system to provide the required on-board power. In this paper, a linear brushless doubly fed machine with dual-primary windings and a reluctance secondary mover is proposed as a means of providing decoupled traction and on-board power. The machine primary contains two three-phase windings with different number of poles while an additional third winding is added around rotor saliencies forming a third output electric port to provide the required on-board power. A prototype machine is designed and simulated using 2D finite element analysis to verify the proposed concept.

1 Introduction

Today's advanced electric rail systems can be classified into two main categories: those propelled using linear motors; and ones that utilize a rotary propulsion option. Linear electrical motors offer tremendous advantages over rotary types in transportation systems as the mechanical gear and the required transmission systems are dispensed with, resulting in higher efficiency, improved dynamic performance, and improved reliability [1]. Additionally, the inherently orthogonal forces which are excited by linear motors can be also used to support a vehicle [1].

Of the different motor types, induction and PM synchronous machines are the most commonly used types of linear machines. Linear induction machines with a short stator are characterized by lower overall system capital cost and lower maintenance [2, 3]. However, they are typically employed in low-speed systems. On the other hand, PM linear synchronous motors with a long stator are normally used in high speed and long distance transportation systems [4].

In conventional systems, the on-board power is traditionally fed from a catenary system. However, today's trendy cities have opted for catenary-less rail transport. Hence, the alternative is additional power rails placed between the running rails. One rail provides on-board power, and the other provides traction [5]. An example of this technology is the Bombardier Advanced Rapid Transit system based on the company's LIM technology. The need for propulsion and on-board power is a functional requirement in other applications. A rotary antenna used in radar systems is an example where this need arises. In [6], a proposed solution to this application has been analysed, where a rotary mixed pole induction machine was found to provide decoupled rotary torque and electrical power to the rotor mounted electrical load. Brushless doubly fed machines (BDFM), or mixed pole machines (MPM), have generally two stator windings wound with dissimilar pole numbers and a specially designed rotor [6]-[7]. Generally, there are two rotor types, namely, nested cage and reluctance rotor types [6]. Functionally, one winding is designated as the main winding or the power winding with a number of poles $2p_1$, and the other winding is called the control winding with a number of poles $2p_2$. In [6], [7], an n-phase winding is added to a reluctance type rotor to provide an extra electric power port to supply a shaft-mounted rotor. In the literature, the 8/4 pole combination has shown promise in many applications [8]. In [9], a new form of traction drive based on a BDFM is introduced.

The main functional need addressed by this paper is the capability of developing not only a contact-free propulsion system, but also contactless power transfer to the moving active part. This transferred power can be used to feed the electrical loads on the moving train. Hence, a linear MPM (LMPM), analogous to the rotary version introduced in [6, 7], is proposed. The proposed machine primary (stator in the rotary version) is furnished with two single-layer balanced three-phase windings of conventional design, with a dissimilar number of poles. A reluctance secondary (rotor in rotary version) with $p_1 + p_2$saliencies is used. Each saliency is equipped with an n-phase concentric winding. The number of phases equal the number of rotor saliencies. By controlling the winding currents of both primary windings, the machine can provide decoupled transitional mechanical and electrical output powers. A prototype machine with 8/4 stator winding pole combination is designed. The corresponding number of rotor saliences will be six. The rotor winding is wound in such a way to provide a three-phase output terminal. The finite element method is used to verify the proposed design.

2 Theory of Operation

The MPM has two windings with different numbers of pole pairs p_1 and p_2. One winding (arbitrarily) is considered the

Authorized licensed use limited to: Qatar University. Downloaded on March 27,2022 at 06:59:41 UTC from IEEE Xplore. Restrictions apply.

main winding, and the other is the control winding [10], [11]. The main winding is connected directly to the mains or to a power converter. However, the control winding is connected to an inverter with a fraction of the power compared to the machine rated power [12], [13]. This control winding is used to control the machine speed. For doubly-fed operation, the machine operates at a synchronous speed given by [14].

$$\omega_m = \frac{\omega_1+\omega_2}{p_1+p_2} \quad (1)$$

where, ω_m is the angular rotor speed, and
ω_1 and ω_2 are angular frequency of the two stator windings.

The synchronous speed corresponding to zero control winding frequency is called the rated synchronous speed [14]. MPM operation relies on the interaction between the two stator fields through a specially designed rotor. A reluctance rotor with saliencies that are equal to $p_1 + p_2$ provides mutual coupling between the two stator windings [6]; hence, a mechanical torque can be produced. The mutual coupling between the two stator windings depends on the ratio of the rotor pole arc to the rotor pole pitch, which is equal to $2\pi/(p_1 + p_2)$. Adding a winding to the rotor saliencies results in n-phase voltages induced in the n rotor phases shifted in time by $2\pi/n$ rad, where n is equal to the number of saliencies. For a triple number of saliences, different coils can be connected in such a way to produce a balanced three-phase output voltage. Generally, the frequency of the induced rotor voltage, ω_r, is determined by [7]

$$\omega_r = \omega_1 - p_1\omega_m = -\omega_2 + p_2\omega_m \quad (2)$$

Equations (1) and (2) can be used to calculate the two stator winding frequencies for a required machine speed and a desired rotor output frequency, whereas controlling the winding currents controls the magnitude of the total magnetomotive force (MMF). Hence, the magnitude of the three-phase rotor output voltages can be controlled.

The linear MPM will have the same construction and functionally operate with the same concept as the rotary machine. The proposed LMPM is expected to provide the following advantages [10]:

- Synchronous operation: The LMPM operates at a precise speed; the need to calculate the appropriate slip frequency as in a conventional LIM is not an issue. This can simplify vehicle location controls.
- Limp-home capability: LIM propulsion systems need the control of the power conditioning units (PCU) at all times. This leads to a requirement for redundancy in the form of double PCUs or vehicles. On the other hand, the LMPM will operate as a crude induction machine without its PCU; this enables a single PCU vehicle to operate in a degraded mode and return its passengers to the next station in the event of a failure.
- AC vehicle electrics: on board AC power can be utilized.

However, the main disadvantage of the proposed LMPM is its larger size when compared with conventional LIM and LSM. However, this extra cost may be compensated by the saving caused by removing the additional rail used for on-board power transmission.

3 Prototype Machine Design

Since linear motors operate in the same way as their rotary counterparts if the latter is sliced open and laid flat, this section will utilize a machine structure that is similar to the rotary system in order to simplify system development and limit system cost. The proposed architecture is shown in Fig. 1. A full rotary stator is utilized, however, in order to account for the end effect problems associated with linear machines, an electromagnetic equivalent is suggested. The proposed experimental prototype utilizes half a rotor, and replaces the remaining rotor magnetic circuit with a non-magnetic filling material. The non-magnetic half rotor is utilized to help maintain mechanical symmetry and does not provide any magnetic function. A slip-ring/brush assembly is used to extract electrical power from the rotor. The machine stator in Fig. 1 is equivalent to a long stator in linear version, while the rotor and the added rotor winding represent the mover and the additional on-board electric port.

For simplicity, the stator is wound with two single layer windings. The lower layer comprises an 8-pole winding and the upper layer provides a 4-pole winding. The 4-pole winding will be considered as the power winding, while the 8-pole winding will be the control winding. To improve MMF distribution, it is better to employ double layer winding with suitable chording to reduce the magnitude of the low order harmonics. For this winding layout and for this pole-pair combination, the selected number of slots will be 24. Since the active machine length equals half the total peripheral length, as shown in Fig. 1, the total number of slots in the whole stator, which represents a linear machine with long stator, will be 48 slots.

The stator outside radius	103.5mm
The inner stator arc radius	65.5mm
The stack length	100mm
The active machine peripheral length	205.8mm
Stator teeth width	4.2mm
Air gap length	1mm
Rotor slot depth	20mm
Stator slot depth	27mm
Stator back iron	10mm
Number of active stator slots	24
Number of rotor saliences	6
Number of turns per coil (8-pole winding)	75
Number of turns per coil (4-pole winding)	40
Number of turns per coil (Rotor winding)	200
The conductor diameter of the stator winding	0.7mm
The conductor diameter of the rotor winding	0.5mm

Table 1: Prototype machine design specifications.

Authorized licensed use limited to: Qatar University. Downloaded on March 27,2022 at 06:59:41 UTC from IEEE Xplore. Restrictions apply.

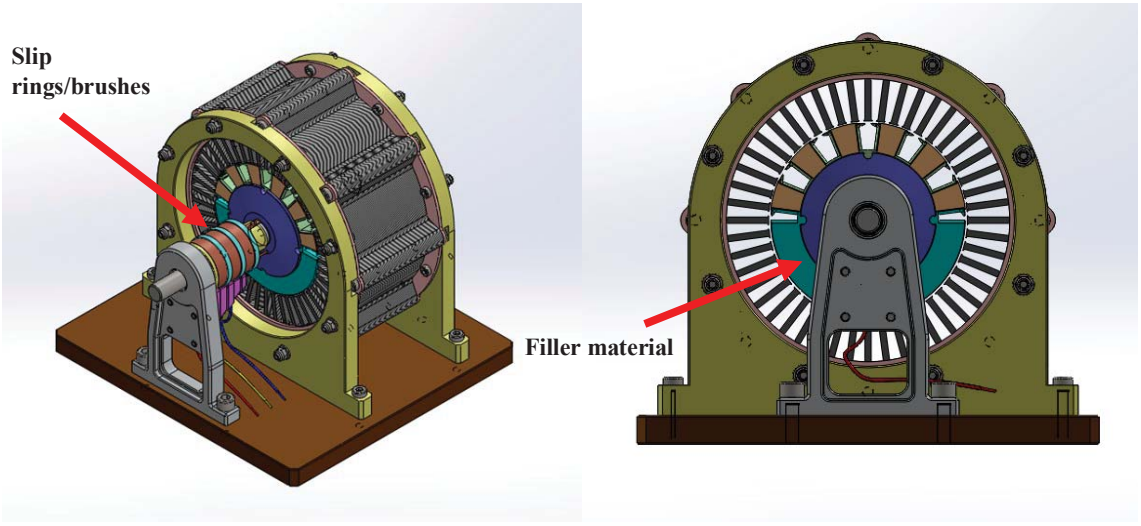

Figure 1: Proposed experimental prototype structure.

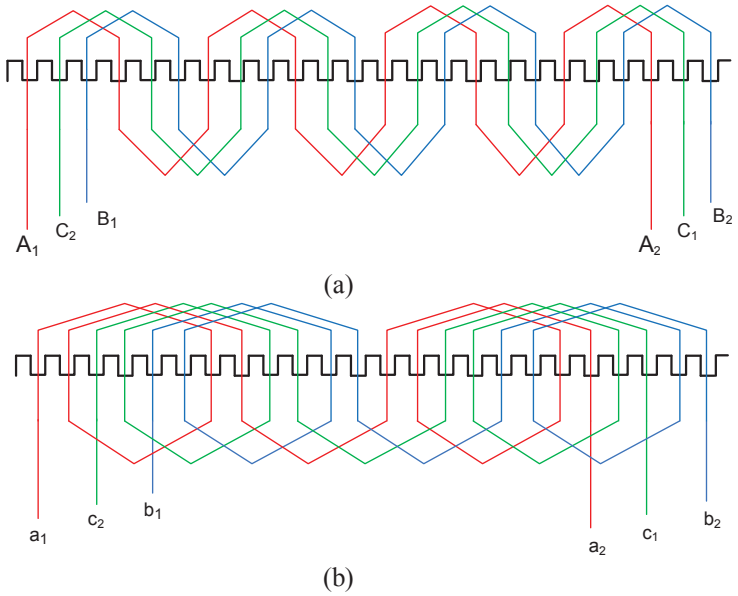

Figure 2: Proposed primary winding layout. (a) 8-pole winding (b) 4-pole winding.

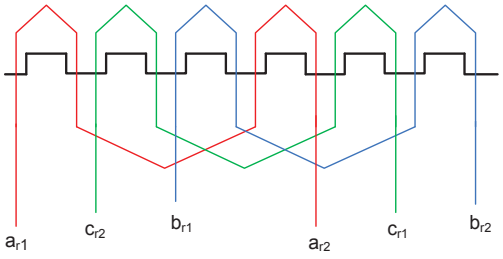

Figure 3: Proposed rotor winding layout.

Since, the machine design is a bit tricky [15], it will be started by setting certain specifications, and based on steady state circuits, calculated machine inductances and resistances as functions of the number of turns per phase for each winding; the optimum numbers of turns for both windings are selected. The approach is similar to that in [7]. The proposed machine should have the maximum mutual inductance between the two stator windings to maximize the machine torque production, as claimed in [7]. This is to increase the thrust component F_{12} due to the interaction between the two stator winding currents. This force component depends mainly on the mutual inductance M_{12} between the two stator windings and the stator winding currents. This mutual inductance depends on the rotor pole arc to pole pitch ratio. The selected value for this ratio is 0.5, which maximizes the mutual inductance, as detailed in [7].

Both stator windings are wound with the same copper conductor diameter of 0.7mm. The corresponding rated current for both windings will be 4A. For a total number of 24 slots, the number of slots per pole per phase for the 4-pole winding is 2 and for the 8 pole winding is 4. The corresponding winding layout for both windings of the half stator is shown in Fig. 2. This winding layout is repeated twice around the stator periphery.

For the selected number of stator pole pairs, the required number of rotor saliences will be 6, as shown in Fig. 1, and the corresponding rotor winding layout to provide three-phase terminals is shown in Fig. 3. Each two coils are connected in series to form one phase. The selected number of turns for each coil is 200 turns. This gives a total number of turns per

Authorized licensed use limited to: Qatar University. Downloaded on March 27,2022 at 06:59:41 UTC from IEEE Xplore. Restrictions apply.

phase equal to 400 turns. The selected conductor diameter of the rotor winding is 0.5 mm. Assuming a current density of 7 A/mm^2, this makes the windings capable of carrying a current of 1.5 A. The three-phase rotor windings are star connected and the tree-phase terminals are connected to three slip rings as in Fig. 1 for terminal provision. In an actual system, these slip rings are not necessary. The detailed design parameters for the prototype machine are given in Table 1.

4 Simulation results

The designed machine is simulated using finite element simulation using the JMAG-studio10 program. The 4-pole winding is connected to a three-phase current of 4A (rms) and a frequency of 6Hz. The 8-pole winding is connected to a DC source, whereas phase "a" is connected to the positive terminal, and phases "b" and "c" are both connected to the negative terminal. The 8-pole winding is held constant at 4A. The corresponding linear synchronous secondary speed is 0.21m/s. The rotor initial position is set such that the maximum mechanical thrust is produced. The secondary circuit is connected to a three-phase rectifier to produce a DC output power to the secondary circuit. The rectifier output is connected to a 50Ω resistive load.

The machine flux distribution is shown in Fig. 4, while the corresponding air gap flux distribution is given in Fig. 5. For the maximum loading conditions, the flux distribution falls within the acceptable iron saturation limits, as depicted by Fig. 4.

The simulation results for different machine variables are shown in Fig. 6. The phase currents for both stator (primary) windings are shown in Figs. 6a and 6b, while the corresponding phase voltages are shown in Figs. 6c and 6d respectively. The induced rotor (secondary) voltages are illustrated in Fig. 6e, the corresponding phase currents are shown in Fig. 6f, and the rectifier DC voltage output is given in Fig. 6g. The machine thrust for this loading condition is given in Fig. 6h. The relatively high thrust ripple is mainly caused due to both spatial harmonics, slotting effect, and the rotor current harmonics due to diode commutation. The prototype machine used has a unity number of slots/pole/phase which corresponds to a relatively distorted airgap flux distribution, as shown in Fig. 5. The airgap flux distribution can be improved by proper winding design. Moreover, employing a PWM voltage source rectifier instead of a simple diode rectifier enables an improved rotor current waveform and hence smaller induced thrust ripple. Skewing the secondary saliencies stands as another technique to significantly reduce the thrust ripples, however with a corresponding reduction in the average machine thrust. A complete design optimization study will be considered in the future wok.

Based on the simulation results along with the complete analysis addressed for the rotary machine version in the earlier work by the authors [6], the proposed machine can successfully provide an output mechanical power at constant synchronous speed while maintaining a decoupled electric output power through rotor terminals. However, a controller similar to that given in [7, 17] should be employed. Experimental results for the prototype system will be provided in future work upon completion with complete characteristic curves.

5 Conclusion

This paper proposes a new linear mixed pole machine with contactless power transfer capability for traction application. The proposed system can provide, if properly controlled, a decoupled mechanical power to drive the train and an electric power through an additional electric output port to feed on-board loads. A 8/4 mixed pole machine with three-phase rotor output is designed and simulated using 2D finite element analysis. Although the simulation results prove the proposed concept, however, a complete system investigation including controller design and experimental investigation is expected in the near future.

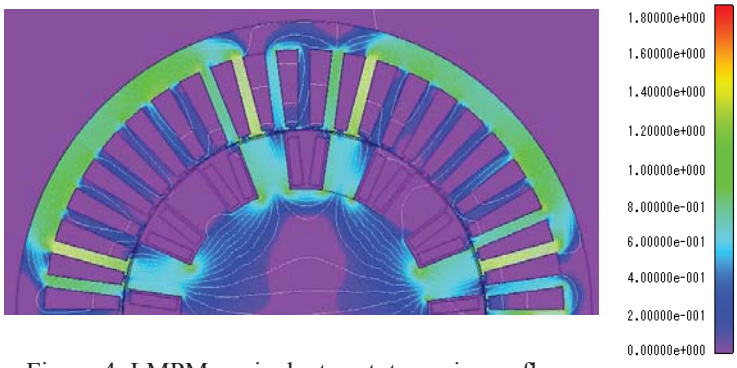

Figure 4: LMPM equivalent prototype air gap flux density and flux density distribution.

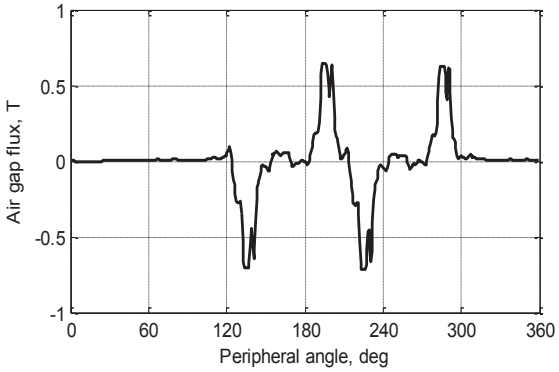

Figure 5: Air gap flux distribution with peripheral angle.

Authorized licensed use limited to: Qatar University. Downloaded on March 27,2022 at 06:59:41 UTC from IEEE Xplore. Restrictions apply.

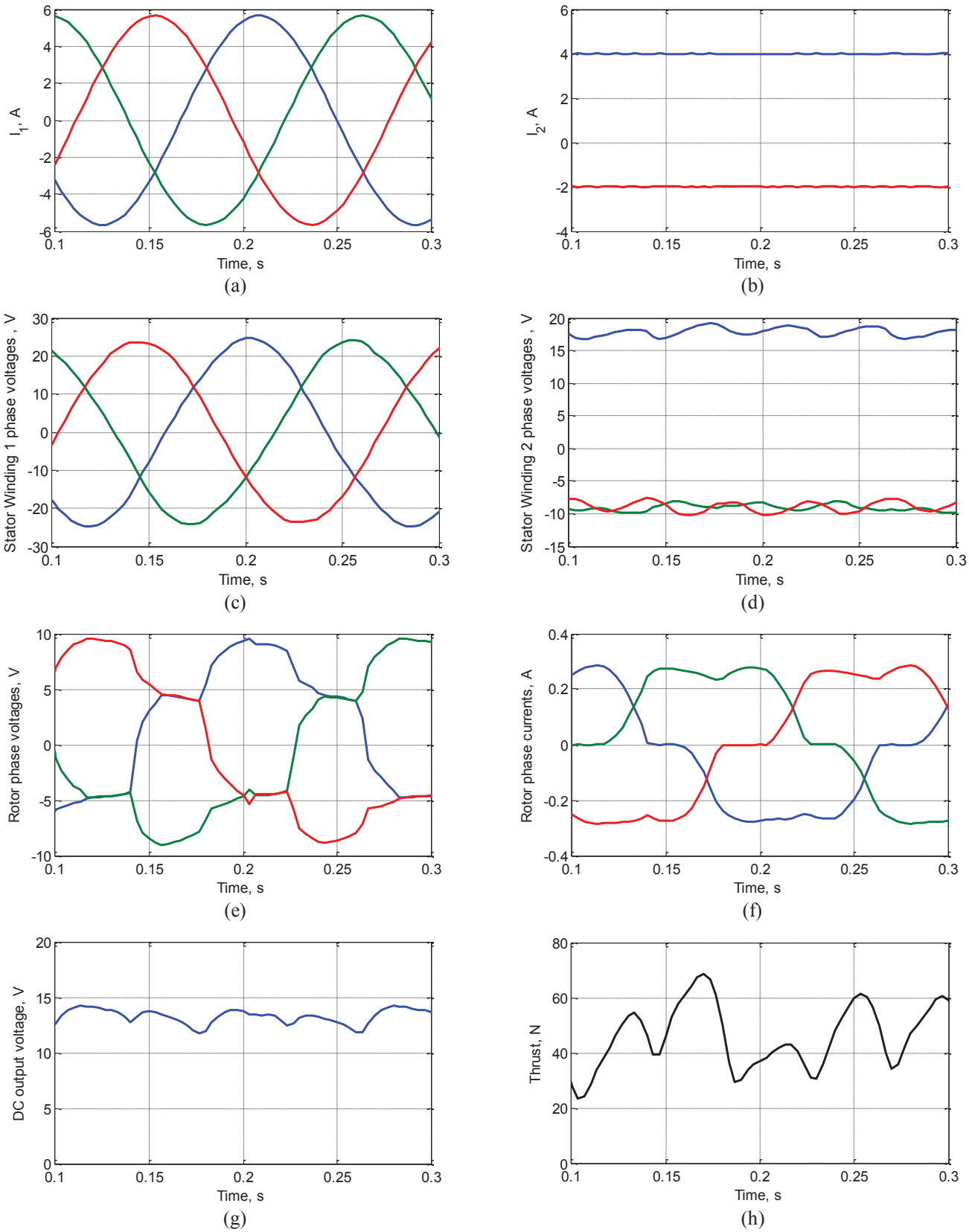

Figure 6: Finite element simulation results. (a) 4-pole winding phase currents. (b) 8-pole winding phase currents. (c) 4-pole winding phase voltages. (d) 8-pole winding phase voltages. (e) Rotor winding phase voltages. (f) Rotor winding phase currents. (g) Rotor DC output voltage. (h) Machine developed thrust.

Authorized licensed use limited to: Qatar University. Downloaded on March 27,2022 at 06:59:41 UTC from IEEE Xplore. Restrictions apply.

Acknowledgements

This publication was made possible by NPRP grant [09 - 1001 - 2 – 391] from the Qatar National Research Fund (a member of Qatar Foundation). The statements made herein are solely the responsibility of the authors.

References

[1] R. Hellinger, P. Mnich. "Linear motor-powered transportation: history, present status, and future outlook", *Proceedings of the IEEE*, **volume** 97, no. 11, pp. 1892-1900, (2009).

[2] T. Morizane, K. Tsujikawa, N. Kimura. "Control of traction and Levitation of linear induction motor driven by power source with frequency component synchronous with the motor speed", *IEEE Trans. Magnetics*, **volume** 47, no. 10, (2011).

[3] W. Xu, J. Zhu, Y. Zhang, Y. Li, Y. Wang, Y. Guo. "An improved equivalent circuit model of a single-sided linear induction motor", *IEEE Trans. Vehicular Technology*, **volume** 59, no. 5, pp. 2277-2289, (2010).

[4] K. Suzuki, Y. Kim, H. Dohmeki. "Driving method of Permanent-magnet linear synchronous motor with the stationary discontinuous armature for long-distance transportation system", *IEEE Trans. Ind. Electron.*, **volume** 59, no. 5, pp. 2227-2235, (2012).

[5] http://en.wikipedia.org/wiki/Bombardier_Advanced_Rapid_Transit

[6] A. Abdel-Khalik, M. Masoud, B. Williams, A. Mohamadein, M. Ahmed. "Steady-state performance and stability analysis of mixed pole machines with electromechanical torque and rotor electric power to a shaft-mounted electrical load", *IEEE Trans. Ind. Electron.*, **volume** 57, no. 1, pp. 22-34, (2010).

[7] A. Abdel-Khalik, M. Masoud, A. Mohamadein, B. Williams, M. Ahmed. "Control of rotor torque and rotor electric power of a shaft-mounted electrical load in a mixed pole machine", *Proc. IET Electr. Power Appl.*, **volume** 3, no. 4, pp. 265-278, (2009).

[8] S. Shao, E. Abdi, R. McMahon. "Low-cost variable speed drive based on a brushless doubly-fed motor and a fractional unidirectional converter", *IEEE Trans. Ind. Electron.*, **volume** 59, no. 1, pp. 317-325, (2012).

[9] F. Saifkhani, A. K. Wallace. " A linear brushless doubly-fed machine drive for traction applications", *Power Electronics and Applications Fifth European Conference*, **volume** 5, pp. 344-348, (1993).

[10] J. Poza, E. Oyarbide, D. Roye, M. Rodriguez. "Unified reference frame dq model of the brushless doubly fed machine", *Proc. Electr. Power Appl.*, **volume** 153, no. 5, pp. 726–734, (2006).

[11] A. C. Ferreira, S. Williamson. "Time-stepping finite-element analysis of brushless doubly fed machine taking iron loss and saturation into account", *IEEE Trans. Ind. Appl.*, **volume** 35, no. 3, pp. 583–588, (1999).

[12] H. A. Toliyat. "Recent advances and applications of power electronics and motor drives—Electric machines and motor drives", *in Proc. 34th Annu. Conf. IEEE IECON*, pp. 34–36, (2008).

[13] B. K. Bose. "Power electronics and motor drives recent progress and perspective", *IEEE Trans. Ind. Electron.*, **volume** 56, no. 2, pp. 581–588, (2009).

[14] R. McMahon, P. Roberts, X. Wang, P. Tavner. "Performance of BDFM as generator and motor", *Proc. Electr. Power Appl.*, **volume** 153, no. 2, pp. 289–299, (2006).

[15] A. Knight, R. Betz, D. Dorell. "Design and analysis of brushless doubly fed reluctance machines", *IEEE Tran. Ind. Appl.*, **volume** 59, no. 1, pp. 50-58, (2013).

[16] D. Dorrell, A. Knight, R. Betz. "Issues with the design of brushless doubly-fed reluctance machines: Unbalanced magnetic pull, skew and iron losses", in Conf. IEMDC'11, pp. 663-68, (2011).

[17] A. Abdel-khalik, M. Masoud, A. Mohamadein, B. Williams, M. Ahmed. "Control of rotor torque and rotor electric power in a reluctance wound rotor brushless doubly fed machine", *IEEE Power & Energy Society General Meeting* PES '09, pp. 26 – 30, (2009).

Authorized licensed use limited to: Qatar University. Downloaded on March 27,2022 at 06:59:41 UTC from IEEE Xplore. Restrictions apply.